Asymptotic analysis of a killing problem arising in multiscale systems*

R. E. Lee DeVille†

June 19, 2009

Abstract

We consider a class of killing problems with a small parameter and describe a method to develop asymptotic approximations for the value of the process at the killing time. We elucidate the connection between this class of killing problems and calculations of rare events in multiscale systems. Finally, we explain how this class of problems connects to applications in biophysics.

Keywords: Self-induced stochastic resonance, Stochastic resonance, Killing, Large deviations, Multiscale asymptotics, Molecular motors, Gumbel distribution, Fisher-Tippett distribution, Extreme Value distribution

1 Introduction

We consider a specific class of one-dimensional killing problems which include a small parameter in both the diffusion and the killing rate, and develop asymptotic approximations for the value of the diffusion at the killing time. We give a precise statement of the problem in Section 1.1 and give two motivating applications in Section 1.2.

1.1 Problem formulation

Let X_t^ϵ be a solution to the SDE given by

$$dX_t^\epsilon = b(X_t^\epsilon)\,dt + \sqrt{\epsilon}\sigma(X_t^\epsilon)\,dW_t, \quad X_0 = x_0, \quad X_t \in \mathbb{R}, \tag{1}$$

and define an infinitesimal "killing rate":

$$\kappa(x) = \nu(x)e^{\rho(x)/\epsilon}, \tag{2}$$

where $b, \sigma, \nu, \rho \colon \mathbb{R} \to \mathbb{R}$ are C^1, $b(x) > b_* > 0$, $\nu(x) > \nu_* > 0$, $\rho'(x) > 0$, and $0 < \epsilon \ll 1$. Consider a random variable $\zeta > 0$ — the "killing time" — whose law is given by

$$\lim_{\Delta t \to 0} (\Delta t)^{-1}\mathbb{P}(\zeta < t + \Delta t | \zeta \geq t) = \kappa(X_t^\epsilon),$$

*submitted to *Journal of Statistical Physics*

†Department of Mathematics, University of Illinois, Urbana IL 61801, rdeville@illinois.edu

and we are interested in characterizing the random variable X_ζ^ϵ asymptotically as $\epsilon \to 0$. We are not interested so much in the killing time ζ as X_ζ^ϵ, the **location** of the diffusion at the killing time.

Specifically, in this paper we show how to compute $m_{p,j}$, $p = 1, 2, \ldots, j = 0, 1, 2, \ldots,$ so that the following asymptotic series are well-formed:

$$\mathbb{E}^{x_0}[X_\zeta^\epsilon] = \sum_{j=0}^{n} \epsilon^j m_{1,j}, \tag{3}$$

$$\mathbb{E}^{x_0}[(X_\zeta^\epsilon - \mathbb{E}^{x_0}[X_\zeta^\epsilon])^p] = \sum_{j=0}^{n} \epsilon^j m_{p,j}, \quad p > 1. \tag{4}$$

In this problem we have chosen $b(x), \rho'(x)$ positive. Since the drift $b(x)$ is positive, the diffusion tends to move to the right ($\mathbb{E}^{x_0}[X_t^\epsilon]$ is increasing in t), and notice that the killing rate is designed so that as X_t^ϵ increases, it becomes much more likely to be killed. It is not hard to see that $\mathbb{P}^{x_0}(\zeta < \infty) = 1$. All in all, this can be thought of as a prototypical example of a problem where a diffusion moves a particle towards regions where it is significantly more likely to be killed. Because of this combination, it will not be surprising to note that the probability distribution of the killing location drops off very rapidly in the positive-x direction; in fact, as we show in Section 3, it decays as an iterated exponential.

Finally, we remark on one surprising result from this analysis. It turns out that increasing the amplitude of the noise makes a significant contribution to the mean of X_ζ^ϵ without changing its variance very much. This is, of course, the exact opposite of what happens for the mean and variance of X_t^ϵ, and is due to the strong spatial dependence of the killing rate.

1.2 Motivation/Applications

1.2.1 Molecular motors

Motor proteins are nanometer-sized engines capable of generating motion at the microscopic level (for reviews see e.g. [2, 30]). Many different types of motor proteins exist in eucaryotic cells; these proteins move various organelles and vesicles from one place to another. Other types of motor proteins are also responsible for cell division and muscle contraction. Typically, motor proteins bind to filament tracks made of actin or microtubules, and move along them using the energy generated by hydrolysis (and thus the motion of the motor can be modeled by a one-dimensional process). The part of the motor protein which binds to the track is called the “motor head”, and this is the part of the motor which hydrolyzes ATP. The rest of the protein is referred to as the “tail domain”; it is this part of the protein which binds to the load on which the motor protein performs work. The hydrolysis process is part of a complicated cycle during which the motor protein experiences conformational changes together with binding and unbinding to the track, the net effect of which is the motion by one step along the track (typically one step is a few nanometers long).

A wide variety of mathematical models have been proposed for motor proteins and, consistent with the observation that the motors operate in the thermal bath of the solvent, these models typically have a stochastic component. One particular class of models which has shown a remarkable degree of success is that due to Fisher and Kolomeisky [15, 16, 23]. In this model, the motor is located at a discrete set of sites along its track, and steps forward or backward as a Markov jump process. The rates of the jumps depend on the force applied by the cargo, which in turn depends on the distance between the cargo and the motor. More specifically, when a motor is located at position m, and a cargo at position c, the rate at which a motor "steps forward" is given by the formula

$$\rho(m,c) = \rho_0 \exp(-LF(m-c)/k_B T), \tag{5}$$

where F is the force between cargo and motor, L a characteristic length associated to the motor's step size, k_B Boltzmann's constant, T temperature, and ρ_0 the "zero separation stepping rate". Using the appropriate rescaling (see [11, Appendix A] for details), one can write this as

$$\tilde{\rho}(\tilde{m},\tilde{c}) = \rho_0 \exp(\phi(\tilde{m}-\tilde{c})/\epsilon), \tag{6}$$

where $\epsilon = k_B T/\kappa L^2$ and $\kappa = F'(0)$ is the linear spring constant corresponding to F. We can see for fixed $\tilde{m}$, (6) has precisely the same form as (2). Moreover, the diffusion coefficient of the cargo is $\sqrt{C\epsilon}$ for some fixed constant C (for details of this derivation, see [10, Section 3]), and thus the motion of the cargo is governed by an SDE with the same scalings as (1). The "killing" of the diffusion corresponds to the motor's stepping forward one step, at which time the system is reset with new initial conditions. In practice, this model is in fact a bit more complicated, since there are several conformational changes which can take place at any given time (e.g. the motor can step forward or backward), but in the idealization of there being only one such conformational change, (1, 2) is an good model for the dynamics of a motor-cargo complex.

For the parameters corresponding to the specific protein myosin-V, the nondimensional parameter ϵ is likely in the range $(0.1, 0.6)$ [11, Appendix A]. The author (and collaborators) [11, 12, 10] have shown that the $\epsilon \to 0$ limit gives a reasonably good approximation for the dynamics of a motor-cargo system, which is reasonable since ϵ is "small". However, since ϵ is "not too small", one expects that asymptotic corrections play a role, which directly motivates the current study.

1.2.2 Jumping times for singularly-perturbed SDE

We follow the exposition of [8] in describing the phenomenon of *self-induced stochastic resonance*, first identified in [25] (see also [17]). Consider the singularly-perturbed SDE:

$$dx = f(x,y)\,dt + \sqrt{\epsilon}h(x,y)\,dW_t^{(x)}, \tag{7}$$

$$dy = \alpha g(x,y)\,dt + \sqrt{\alpha\epsilon}k(x,y)\,dW_t^{(y)}, \tag{8}$$

where $0 < \alpha, \epsilon \ll 1$, $f, g, h, k \in C^2$, and h is uniformly bounded below, $x \in \mathbb{R}^n, y \in \mathbb{R}$. Here we have n "fast" variables and 1 "slow" variable (this would typically be called a $n+1$-dimensional system).

If we consider no noise ($\epsilon = 0$), this problem is the classical singularly perturbed ODE. For simplicity of exposition, assume that there exists an interval $I \subset \mathbb{R}$, so that for each $y \in I$,

$$\frac{dx}{dt} = f(x,y)$$

has a finite number of attracting fixed points and that the closure of the union of their basins of attraction is all of $\mathbb{R}^n$. We will index these as $x_1(y), \ldots, x_n(y)$, and these are all smooth functions on some subinterval of I by the Implicit Function theorem (of course any may fail to be defined for some $y \in I$), and these define smooth 1-D submanifolds of R^{n+1}. We denote these as S_i. (These are typically called "slow manifolds".) If $\epsilon = 0$, the system is deterministic, and after a rescaling of time we obtain the system

$$\begin{aligned} \alpha \frac{dx}{dt} &= f(x,y), \\ \frac{dy}{dt} &= g(x,y). \end{aligned} \tag{9}$$

From standard results in singular perturbation theory [29, 27, 31], we know that the trajectories of (9) will spend most of their time tracking the S_i, and the evolution is given by the slow variables restricted to the slow manifold. (More precisely, it can be shown that the trajectories typically lie in an $O(\alpha)$ neighborhood of the slow manifolds.) The system will switch between different slow manifolds when the trajectory "falls off" one of them.

Now consider the case with noise ($\epsilon > 0$). It is now possible for a trajectory to leave a neighborhood of a slow manifold much earlier than it would in the deterministic system, because the noise can kick it away. If we consider (7) with y fixed, we now have a system with several attracting fixed points perturbed by noise, and we know that (7) will spend an exponentially-large proportion of time near these fixed points, but on long timescales, can switch between the two.

Fix $\alpha = 0$, and for each ϵ, y, we define $\tau_{ij}^{\epsilon}(y)$ as the time it takes to switch between S_i and S_j. More specifically, choose some neighborhoods N_i, N_j around $x_i(y), x_j(y)$, and define

$$\tau_{ij}^{\epsilon}(y) := \inf_{t>0} \{t : X_t^{\epsilon} \in N_j \text{ given that } X_0^{\epsilon} \in N_i\}.$$

(Notice that since $\alpha = 0$, y is fixed.) Of course, this escape time will depend on the choice of neighborhoods, but one of the main results of the Wentzell-Freidlin large deviation theory [18] is that there exists an "action" $I_{ij}(y) > 0$ such that

$$\lim_{\epsilon \to 0} \epsilon \log \tau_{ij}^{\epsilon}(y) = I_{ij}(y),$$

independent of the choice of neighborhoods as long as they are small enough (in fact, as long as they are compactly contained in the basins of attraction of the corresponding fixed points). The computation of this action is relatively standard but can be complicated in general (see [18] for details). However, one straightforward case is the case of gradient flow: if $f(x,y) = -\nabla V_y(x)$ is the gradient of a potential for each fixed y, and the basins of attraction of $x_i(y), x_j(y)$ share a boundary, then choose x_s, the saddle point on this boundary with lowest potential, and then

$$I_{ij}(y) = V(x_s) - V(x_i(y)).$$

If we consider a solution of (7) with initial condition near $x_i(y)$, then the most likely switch of basins will be to a neighborhood of $x_{j^*}(y)$, where

$$j^*(i,y) := \arg\min_j I_{ij}(y),$$

and the time it takes will be asymptotically equivalent $e^{I_i(y)/\epsilon}$, where we define $I_i(y) = I_{ij^*(i,y)}(y)$.

All of the above is for y fixed, but since $\alpha > 0$, y is slowly-varying as well. The combined problem was originally studied in [17, 25], where it was shown that if we consider the limit

$$\epsilon \log \alpha^{-1} \to \beta > 0, \tag{10}$$

then trajectories near S_i will move along S_i under the restricted dynamics until such time that $I_i(y) \leq \beta$, at which time the trajectory jumps to a neighborhood of $S_{j^*(i,y)}$.

To see why this should be true, notice that if $I_i(y) > \beta$, then the time it takes the fast system to escape a neighborhood of $x_i(y)$ is roughly $e^{I_i(y)/\epsilon} \gg e^{\beta/\epsilon} = \alpha^{-1}$. So the jump timescale of the fast system is much longer than the slow evolution, so we are likely to not see a jump before the slow system changes. On the other hand, if $I_i(y) < \beta$, then $e^{I_i(y)/\epsilon} \ll \alpha^{-1}$, meaning that we are very likely to see a jump before the slow system changes. In particular, if we have a slow manifold S_i such that the slow flow along this manifold is in the direction of decreasing $I_i(y)$, then in the limit (10) the system will move along S_i until it reaches the point where $I_i(y) = \beta$, at which time it will jump to I_{j^*} with probability one.

All of the above is correct in the limit (10); in particular, when we take $\epsilon \to 0$. The next natural question to ask is what the corrections to this jump location are when ϵ is small but positive. Certainly, when ϵ is small, we expect the jump location to be near where it is when $\epsilon = 0$, so we want to develop this location in an asymptotic series around the $\epsilon = 0$ location. The local dynamics near the slow manifold S_i will be, in the absence of jumping away,

$$dy = \alpha G_i(y)\, dt + \sqrt{\alpha\epsilon} K_i(y)\, dW_t^{(y)}, \tag{11}$$

where G_i, K_i can be computed exactly [6] (in fact, K_i is simply the projection of k onto S_i, and G_i is the projection of g onto S_i plus an $O(\epsilon)$ "Itô correction" related to the curvature of S_i). The system will "jump away" from S_i with rate

$$\nu_i(y) e^{-I_i(y)/\epsilon}. \tag{12}$$

Here we have explicitly written down the "prefactor" $\nu_i(y)$ because it plays a role in the asymptotics; in general, this ν_i can be determined from the Kramers-Eyring formula [24, 4]. After rescaling time in (11, 12) by α in the limit (10), we obtain (1) and (2), with $b = G_i, \sigma = K_i, \rho = I_i$.

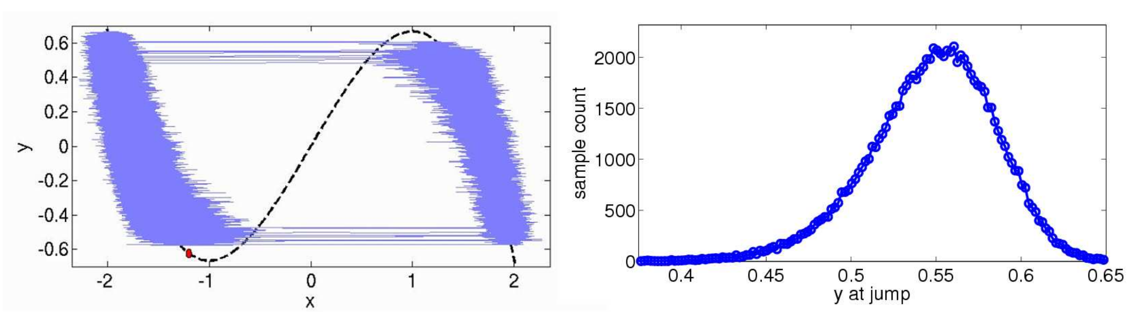

Figure 1: Simulations of (13) with $\epsilon = 0.2, \alpha = 10^{-4}, A = 1.2$. In (a) we plot one realization of (13) in the x, y plane, using an 1st-order Euler method with timestep $dt = 10^{-2}$ and running until $t = 3 \times 10^5$. In (b) we plot a histogram of the value of y when the system jumps away from the right slow manifold (computed over a much longer run).

We show an example in Figure 1. Here consider the SDE

$$\begin{aligned} dx &= x - x^3/3 - y\, dt + \sqrt{2\epsilon}\, dW_t^{(x)}, \\ dy &= \alpha(x + A)\, dt + \sqrt{2\alpha\epsilon}\, dW_t^{(y)}, \end{aligned} \tag{13}$$

where $A = 1.2$. In the absence of noise and for α sufficiently small, this system has a globally attracting fixed point near $(-A, -A + A^3)$. In fact, the system would travel along one of the two stable branches of the cubic nullcline (shown in the figure as a dotted line) — if on the right branch, it would move up until it fell off the "knee" at $(1, 2/3)$ and stop at the red point, and if on the left branch, it would move towards the fixed point. However, it is clear that in the presence of noise, the system undergoes a noisy oscillation, because it is always jumping away from the slow manifold "too soon", but in the limit (10), it can be shown that the system jumps away from the slow manifold in a reliable location (this system is fully analyzed in [8]).

However, this is only true in the limit (10); what happens for finite α, ϵ? In the simulations in Figure 1, we simulate this system for $\epsilon = 0.2, \alpha = 10^{-4}$. We can see that while the system does not jump completely reliably, the jump locations have a relatively small variance. To get an estimate of the jump locations, we can use the theory developed in Section 3 below, if we replace the fast process with a jump process whose rate is given by (12). That calculation predicts that the location of the jump away from the right manifold has a mean of 0.558 and a standard deviation of 5.13×10^{-2}. The empirically-determined mean and standard deviation (from the data displayed in Figure 1) are 0.547 and 6.19×10^{-2}. This is a reasonably good approximation at least for the mean, giving less than 2% error, although the standard deviation is off by about 20%.

However, even though in this case the approximation works relatively well, we note that we have made an uncontrolled approximation for the jump times of (7, 8): we have assumed that (12) is exact and that the probabilities of jumping at each y are independent, and the latter in particular is only true in the limit — in fact, for $\epsilon > 0$ the fast system has a memory, e.g. if an excursions almost occurs for the fast variables, this makes future excursions more likely for some ϵ-dependent time. To take all of these dependencies, and corrections to the rate, into account requires an analysis comparable to that done in [9]; the dependence in particular adds significant complication to the theory. We leave the full solution for future work.

1.3 Organization of paper

The remainder of this paper is organized as follows. In Section 2 we first present the simpler case of $\sigma \equiv 0$ in 1 (cf. a similar calculation already performed in [7]), and in Section 3 we demonstrate the method to solve the problem in full generality. Finally, in Section 4 we compare the asymptotic expansions with direct numerical simulations of the killing problem.

2 Deterministic slow subsystem

Let us first consider the simpler case of (1, 2) where we chose $\sigma \equiv 0$, so that the diffusion is replaced by an ODE. Define the cumulative probability distribution $P(t) = \mathbb{P}(\zeta > t)$. Then

$$\frac{dP}{dt} = -P(t)\nu(y(t))e^{\rho(y(t))/\epsilon} \tag{14}$$

and changing variables with respect to y, using $dy/dt = b(y)$, we get

$$\frac{dP}{dy} = -P(y)\frac{\nu(y)e^{\rho(y)/\epsilon}}{b(y)}. \tag{15}$$

Solving for $P(y)$, using the boundary condition that $P(-\infty) = 1$, gives

$$P(y) = \exp\left(-\int_{-\infty}^{y} \frac{\nu(z)}{b(z)} e^{\rho(z)/\epsilon}\, dz\right). \tag{16}$$

Let us first check the limit as $\epsilon \to 0$. Define y_0 such that $\rho(y_0) = 0$. If $y < y_0$, then the exponent in the inner exponential is negative for all z in the domain of integration, and thus the integrand is exponentially small, meaning that $P(y) \to 1$. Similarly, if $y > y_0$, then for some z in the domain of integration, the exponent in the inner exponential is positive for some of the domain. Therefore the integrand is exponentially large, making the integral exponentially large, meaning $P(y) \to 0$. So we have

$$\lim_{\epsilon \to 0} P(y) = \begin{cases} 1, & y < y_0, \\ 0, & y > y_0. \end{cases}$$

In the limit, P is a Heaviside function which jumps at the zero of ρ. Now we compute the $O(\epsilon)$ asymptotics for $\epsilon > 0$. Recall (15) and consider the expansion

$$y = y_0 + \epsilon(z + z_0), \tag{17}$$

where z_0 remains to be determined and $\rho(y_0) = 0$. Changing variables in (15) gives

$$\begin{aligned} \frac{dP}{dz} &= -\epsilon \frac{P(z)\nu(y_0 + \epsilon(z + z_0))}{b(y_0 + \epsilon(z + z_0))} e^{-\rho'(y_0)(z+z_0)+O(\epsilon)} \\ &= -\epsilon P(z) \frac{\nu(y_0 + \epsilon z_0)}{b(y_0 + \epsilon z_0)} e^{\rho'(y_0)z} e^{\rho'(y_0)z_0}. \end{aligned} \tag{18}$$

We want to choose z_0 to match powers of ϵ, namely

$$e^{\rho'(y_0)z_0} = \epsilon^{-1}, \quad \text{or } z_0 = \frac{\log \epsilon^{-1}}{\rho'(y_0)},$$

so we expand around

$$y^* = y_0 + \epsilon z_0 = y_0 + \frac{\epsilon \log \epsilon^{-1}}{\rho'(y_0)}.$$

Thus

$$\frac{dP}{dz} = -Ae^{Bz}P(z) + O(\epsilon), \quad A := \frac{\nu(y^*)}{b(y^*)}, \quad B := \rho'(y_0).$$

The "inner expansion" of the cdf is

$$\frac{dP}{dz} = -Ae^{Bz}P(z), \tag{19}$$

where we impose the boundary conditions $P(-\infty) = 1, P(\infty) = 0$. We can solve this by integration to get

$$P(z) = \exp\left(-\int_{-\infty}^{z} Ae^{B\zeta}\, d\zeta\right), \text{ or, } P(z) = \exp\left(-\frac{A}{B}e^{Bz}\right). \tag{20}$$

To compute the moments of the jump, we obtain the pdf by $p(z) = -P'(z)$:

$$p(z) = A \exp\left(Bz - \frac{A}{B}e^{Bz}\right).$$

We define

$$m_1 = \int_{-\infty}^{\infty} xA\exp\left(Bx - \frac{A}{B}e^{Bx}\right)\,dx,$$
$$m_k = \int_{-\infty}^{\infty} (x-m_1)^k A\exp\left(Bx - \frac{A}{B}e^{Bx}\right)\,dx.$$

Using the method in Appendix A, we compute

$$m_1 = -\frac{\gamma + \log(A/B)}{B}, \quad m_2 = \frac{\pi^2}{6B^2}, \quad m_3 = -\frac{2\zeta(3)}{B^3},$$
$$m_4 = \frac{3\pi^4}{20B^4}, \quad m_5 = -\frac{10\pi^2\zeta(3) + 72\zeta(5)}{3B^5}, \quad m_6 = \frac{61\pi^6 + 6720\zeta(3)^2}{168B^6},$$

where $\zeta(\cdot)$ is the Riemann Zeta function and γ is the Euler–Mascheroni constant:

$$\gamma := \lim_{n\to\infty}\left[\left(\sum_{k=1}^{n}\frac{1}{k}\right) - \ln n\right] \approx 0.57722.$$

These can be computed exactly to any order (see Appendix A).

Notice that the third moment is always negative, and all moments higher than one depend only on $|\rho'(y_0)|$ and not ν, b. Let Z be the random variable who cdf is given by (19), and then if Y^ϵ is the location of the jump, then

$$\langle Y^\epsilon\rangle = y_0 + \frac{\epsilon\log\epsilon^{-1}}{|I'(y_0)|} + \epsilon\langle Z\rangle, \tag{21}$$

and

$$\left|(Y^\epsilon - \langle Y^\epsilon\rangle)^k\right| = \epsilon^k\left\langle (Z - \langle Z\rangle)^k\right\rangle. \tag{22}$$

Thus

$$\langle Y^\epsilon\rangle = y_0 + \frac{\epsilon\log\epsilon^{-1}}{\rho'(y_0)} - \epsilon\frac{\gamma + \log(\nu(y^*)/b(y^*)\rho'(y_0))}{\rho'(y_0)} + o(\epsilon),$$
$$\left|(Y^\epsilon - \langle Y^\epsilon\rangle)^2\right| = \epsilon^2\frac{\pi^2}{6\rho'(y_0)^2} + o(\epsilon^2), \quad \left|(Y^\epsilon - \langle Y^\epsilon\rangle)^3\right| = -\epsilon^3\frac{2\zeta(3)}{\rho'(y_0)^3} + o(\epsilon^3), \text{ etc.}$$

3 Stochastic slow subsystem

3.1 Rescaling

We consider (1, 2), where σ can now be nonzero. Performing the same inner expansion as in (17), i.e.

$$y = y_0 + \epsilon(z + z_0) = y^* + \epsilon z, \quad t = \epsilon\tau,$$

gives the rescaled SDE

$$dZ_\tau = b(y^*)\,d\tau + \sigma(y^*)\,dW_\tau + O(\epsilon). \tag{23}$$

The rate rescales as

$$\begin{aligned}\kappa(y)\,dt &= \kappa(y^* + \epsilon z_0)\epsilon\,d\tau \\ &= \nu(y^*)\exp(\rho'(y_0)z_0)\exp(\rho'(y_0)z)\epsilon\,d\tau \\ &= \nu(y^*)\exp(\rho'(y_0)z)\,d\tau.\end{aligned} \tag{24}$$

(We could, of course, exchange y_0 and y^* anywhere; this will only lead to a correction at yet higher order, since $y^* = y_0 + \epsilon\log\epsilon^{-1}$.)

We will write (23, 24) as

$$dZ_t = \mu\,dt + \sigma\,dW_t, \tag{25}$$

$$\kappa(z) = \nu e^{\rho z}. \tag{26}$$

Note that in the rescaled variables, the coefficients of the diffusion no longer depend on space; this simplifies the analysis considerably and allows for the explicit solution we present below.

3.2 Feynman–Kac representation

We extend the state space of Z_t to be the set $\mathbb{R}\cup\{\partial\}$, where ∂ is the "coffin" state where the process goes when it is killed. We denote the killing time as ζ, and we define the process $\tilde{Z}_t$ by

$$\tilde{Z}_t = \begin{cases} Z_t, & t < \zeta, \\ \partial, & t \geq \zeta. \end{cases}$$

Then [26] we have

$$\mathbb{E}^{z_0}[f(\tilde{Z}_t)] = \mathbb{E}^{z_0}[f(Z_t)\chi_{[0,\zeta)}(t)] = \mathbb{E}^{z_0}\left[f(Z_t)\exp\left(-\int_0^t \kappa(Z_s)\,ds\right)\right],$$

where we have used the convention that $f(\partial) = 0$. We can now use the Feynman–Kac formula as follows: let $v(x,t) = \mathbb{E}^{z_0}[f(\tilde{Z}_t)]$, then

$$\frac{\partial}{\partial t}v(x,t)|_{t=0} = Lf(x),$$

where

$$Lf = \frac{\sigma^2}{2}\frac{d^2 f}{dx^2} + \mu\frac{df}{dx} - \kappa(x)f. \tag{27}$$

Unfortunately, we cannot use this formulation directly to compute the quantity we seek. This derivation is very useful in determining the **time** of escape, e.g. we know that

$$\mathbb{P}(\zeta > t) = \int_{\mathbb{R}} v(x,t)\,dx, \tag{28}$$

but it is not itself directly useful in determining the **location** of Z_ζ.

3.3 Green's function

We present a slightly-modified version of the derivations of [20, Sec. 4.11], [3, Chapter 2], [21, Chapter 5], but we explicitly state everything here for completeness. For the diffusion (25) we associate the three measures: the *speed measure* $m(dy)$, the *killing measure* $k(dy)$, and the *scale function* $s(y)$ with the properties that k satisfies:

$$\mathbb{P}^{z_0}(Z_\zeta \in A; \zeta < t) = \int_0^t ds \int_A k(dy) p(s; z_0, y) \tag{29}$$

were $p(t; x, y)$ is the transition density function of the process, and where s, m satisfy $Ms = 0, M^* m = 0$, with

$$Mf = \frac{\sigma^2}{2} \frac{d^2 s}{dx^2} + \mu \frac{ds}{dx}.$$

Solving for m, s, k,

$$m(dy) = \frac{2}{\sigma^2} e^{\frac{2\mu}{\sigma^2} y}\, dy, \quad s(y) = e^{-\frac{2\mu}{\sigma^2} y}, \quad k(dy) = \frac{2}{\sigma^2} \kappa(x) e^{\frac{2\mu}{\sigma^2} y}\, dy. \tag{30}$$

Now consider the eigenvalue problem

$$Lu = \lambda u, u(-\infty) = u(\infty) = 0.$$

Define $\psi_\lambda(y), \phi_\lambda(y)$ to be the increasing (resp. decreasing) eigenfunction which satisfies the left (resp. right) boundary condition. If we define the Green's function

$$G_\lambda(x, y) = \int_0^\infty e^{-\lambda t} p(t; x, y)\, dt,$$

then

$$G_\lambda(x, y) = \begin{cases} W_\lambda^{-1} \psi_\lambda(x) \phi_\lambda(y), & x \le y, \\ W_\lambda^{-1} \phi_\lambda(x) \psi_\lambda(y), & x \le y, \end{cases}$$

where W_λ is the "rescaled Wronskian"

$$W_\lambda := \frac{d\psi_\lambda}{ds}(x) \phi_\lambda(x) - \frac{d\phi_\lambda}{ds}(x) \psi_\lambda(x),$$

and

$$\frac{df}{ds}(x) = \frac{df/dx}{ds/dx}$$

is the Radon-Nikodym derivative. We include the scale function s so that the Wronskian will actually be independent of x [3]. Using (29),

$$\mathbb{E}^{z_0}(f(X_\zeta); \zeta \le t) = \int_0^t ds \int_{\mathbb{R}} k(dy) p(s; x, y) f(y),$$

and using (28), and choosing $f(y) = \chi_{[a,b]}(y)$ this becomes

$$\mathbb{P}^{z_0}(Z_\zeta \in [a, b]) = \int_a^b G_0(x, y) k(dy).$$

Assume, for example, that $z_0 \le a \le b$, and this gives

$$\mathbb{P}^{z_0}(Z_\zeta \in [a,b]) = \int_a^b W_0^{-1}\psi_0(z_0)\phi_0(y)k(dy).$$

Normalizing ϕ_0, ψ_0 so that $W_0 = 1$, we get

$$\mathbb{P}^{z_0}(Z_\zeta \in [a,b]) = \psi_0(z_0)\int_a^b \phi_0(y)k(dy). \tag{31}$$

Let us compute:

$$\begin{aligned}\frac{d}{dx}\frac{d\phi_0}{ds} &= \frac{d}{dx}\left(e^{2\mu x/\sigma^2}\frac{d\phi_0}{dx}\right)\\ &= 2\mu\sigma^{-2}e^{2\mu x/\sigma^2}\frac{d\phi_0}{dx} + e^{2\mu x/\sigma^2}\frac{d^2\phi_0}{dx^2},\end{aligned}$$

and since $L\phi_0 = 0$,

$$\frac{d}{dx}\frac{d\phi_0}{ds}\,dx = 2\sigma^{-2}e^{2\mu x/\sigma^2}\kappa(x)\phi_0(x)\,dx = \phi_0(x)k(dx).$$

Comparing this to (31), we obtain, for $z_0 \le a \le b$,

$$\mathbb{P}^{z_0}(Z_\zeta \in [a,b]) = \psi_0(z_0)\left(\frac{d\phi_0}{ds}(b) - \frac{d\phi_0}{ds}(a)\right). \tag{32}$$

In a similar fashion, if we choose $a \le b \le z_0$, we have

$$\mathbb{P}^{z_0}(Z_\zeta \in [a,b]) = \phi_0(z_0)\left(\frac{d\psi_0}{ds}(b) - \frac{d\psi_0}{ds}(a)\right). \tag{33}$$

The form in which we present the cdf (32, 33) is not convenient for computational purposes, as we would need to renormalize ψ_0, ϕ_0 as we change the endpoint. So, for simplicity, we will only consider the case where we choose $a = z_0$ in (32) or $b = z_0$ in (33). Then the probability density for the escape point is

$$p^{z_0}(Z_\zeta = z) = \begin{cases} A\dfrac{d}{dz}\dfrac{d\phi_0}{ds}(z), & z > z_0,\\[2ex] B\dfrac{d}{dz}\dfrac{d\psi_0}{ds}(z), & z < z_0,\end{cases} \tag{34}$$

where we choose A, B so that $p^{z_0}(z)$ is continuous at z_0 and so that $\int_{-\infty}^{\infty} p^{z_0}(z)\,dz = 1$. This function will be continuous, but not differentiable, at z_0. Finally, note that A, B only need to be computed once for any given z_0.

3.4 Bessel functions

To compute the escape density, we need to compute the functions in the null space of the operator L from (27), i.e. the solutions of

$$\frac{\sigma^2}{2}f'' + \mu f' - \nu e^{\rho x} f = 0. \tag{35}$$

By rescaling space and time we can put this equation in the form

$$\frac{1}{2}f'' + f' + Ae^{Bx}f = 0. \tag{36}$$

If we define $J(\alpha, x)$ as the Bessel function of the first kind which satisfies

$$x^2y'' + xy' + (x^2 - \alpha^2)y = 0,$$

then the solution to (36) is (see Appendix B):

$$f(x) = e^{-x}J(2/B, \sqrt{8AB^{-2}e^{Bx}}).$$

To obtain two independent solutions, we could choose the real and imaginary parts; however, as prescribed above, we want purely increasing and purely decreasing functions. Thus we instead choose the modified Bessel functions (also called the hyperbolic Bessel functions) [1, Sec. 9.6.]:

$$I(\alpha, x) = i^{-\alpha}J(\alpha, ix), \quad K(\alpha, x) = \frac{\pi}{2\sin(\alpha\pi)}(I(-\alpha, x) - I(\alpha, x)),$$

where I is increasing and K decreasing. Undoing the rescaling, we thus choose

$$\phi_0(x) = e^{-\mu x/\sigma^2}K\left(\frac{2\mu}{\rho\sigma^2}, \frac{\sqrt{8\nu e^{\rho x}}}{\rho\sigma}\right), \tag{37}$$

$$\psi_0(x) = e^{-\mu x/\sigma^2}I\left(\frac{2\mu}{\rho\sigma^2}, \frac{\sqrt{8\nu e^{\rho x}}}{\rho\sigma}\right). \tag{38}$$

The large-x asymptotics of I, K are [28, Chapter 5], [22, Chapter 6]:

$$I(\alpha, x) \approx \frac{1}{\sqrt{2\pi x}}e^x, \quad K(\alpha, x) \approx \sqrt{\frac{\pi}{2x}}e^{-x}, x \to \pm\infty, \tag{39}$$

and the small-x asymptotics are

$$I(\alpha, x) \to \frac{1}{\Gamma(\alpha+1)}\left(\frac{x}{2}\right)^\alpha, \quad K(\alpha, x) \to \frac{\Gamma(\alpha)}{2}\left(\frac{2}{x}\right)^\alpha, \quad x \to 0. \tag{40}$$

First check (cf. (32)) that

$$\frac{d}{dx}\frac{d\phi_0}{ds}(x) \to 0, x \to \pm\infty.$$

From (39), we have that

$$\phi_0(x) \approx \exp(-e^{\rho x/2}), x \to \infty,$$

so decays like an iterated exponential for x large. Clearly, even after multiplying this by an exponential and differentiating, this function goes to zero. However, in the other direction, we use (40)

$$\phi_0(x) \approx e^{-\frac{2\mu}{\sigma^2}x}, \quad x \to -\infty.$$

The same asymptotics hold for $\phi_0'(x)$, and from (30), $s'(x) = Ce^{-2\mu x/\sigma^2}$, so that

$$\frac{d\phi_0}{ds}(x) \to C, \quad x \to -\infty.$$

Therefore its derivative goes to zero as $x \to -\infty$.

3.5 Summary

We consider (25, 26) to approximate the location of exit Z_ζ, and from the asymptotic boundary-layer matching, we are interested in studying this random variable in the limit $z_0 \to -\infty$. Using (34), the probability distribution of the escape location (in the rescaled variables) is

$$p(z) := \mathbb{P}^{-\infty}(Z_\zeta = z) = C^{-1}\frac{d}{dz}\frac{d\phi_0}{ds}(z), \tag{41}$$

where C is chosen to make this a probability distribution, i.e.

$$C = \int_{-\infty}^{\infty} \frac{d}{dz}\frac{d\phi_0}{ds}(z)\,dz, \tag{42}$$

and, from (37), (30),

$$\phi_0 = e^{-\mu x/\sigma^2} K\left(\frac{2\mu}{\rho\sigma^2}, \frac{\sqrt{8\nu e^{\rho x}}}{\rho\sigma}\right), \quad s(x) = e^{-2\mu x/\sigma^2}. \tag{43}$$

4 Numerical validation

In all that follows, we compare direct numerical simulation of either (1, 2) or (25, 26) to the asymptotic formulas (41– 43). Our method is as follows: we use a first-order Euler-Muriyama integrator for the SDE with fixed timestep $\varDelta t$; at each step, compute $\kappa(x)\varDelta t$ and $r \in U(0,1)$, and if $r < \kappa(x)\varDelta t$, the process is terminated. We then take an ensemble average of many copies of independent copies of this process. We first simulate (1, 2) directly, using a timestep of $\varDelta t = 10^{-3}$ and taking 10^5 realizations, and present the computation in Figure 2. We took as functions

$$b(x) = \cos(x) + 2, \sigma(x) = 1, X_0^\epsilon = 0, \nu = 3, \rho(x) = 2x^2 - x - 1,$$

and show the results for various values of ϵ. We chose ρ to be increasing and zero at $x = 1$, so that in the limit $\epsilon \to 0$, we expect the system to jump w.p.1 at $x = 1$. To obtain the red curves in this figure, we use (41– 43). For ϵ chosen small enough, the approximation is exact to the eye, and even gives a pretty fair fit for $\epsilon = 1/2$! Finally, one remark: the process which computes the red curve is *completely in closed form* except for one numerical step where we compute the prefactor C in (42).

We next show several simulations in the blown-up variables to show that this method is exact. In our simulations, we consider (25, 26) with $\mu = \nu = \rho = \sigma = 1$, and either choose $Z_0 = -10$ or $Z_0 = 0$. (The latter case is not really relevant for the problem at hand, since the boundary layer matching requires taking initial condition $Z_0 = -\infty$, but it is an interesting case of a non-smooth density and where the piecewise version of (34) is required.) We show these simulations in Figure 3.

Finally, we simulate the process for several values of σ to show the dependence of the first two moments of the jumping time on σ, with all other parameters held fixed; see Figure 4. Here we have chosen $\mu = 1, \nu = 1, \rho = 3$, and $Z_0 = -10$. All simulations take a timestep of $\varDelta t = 10^{-3}$ and an ensemble of 10^5 trials. To obtain the analytic curves we use formulas (41– 43) for $\sigma > 0$ and (21, 22) for $\sigma = 0$.

An interesting observation is that while both of the first two moments of the escape are monotonically increasing functions of σ, the mean changes dramatically, while the standard deviation

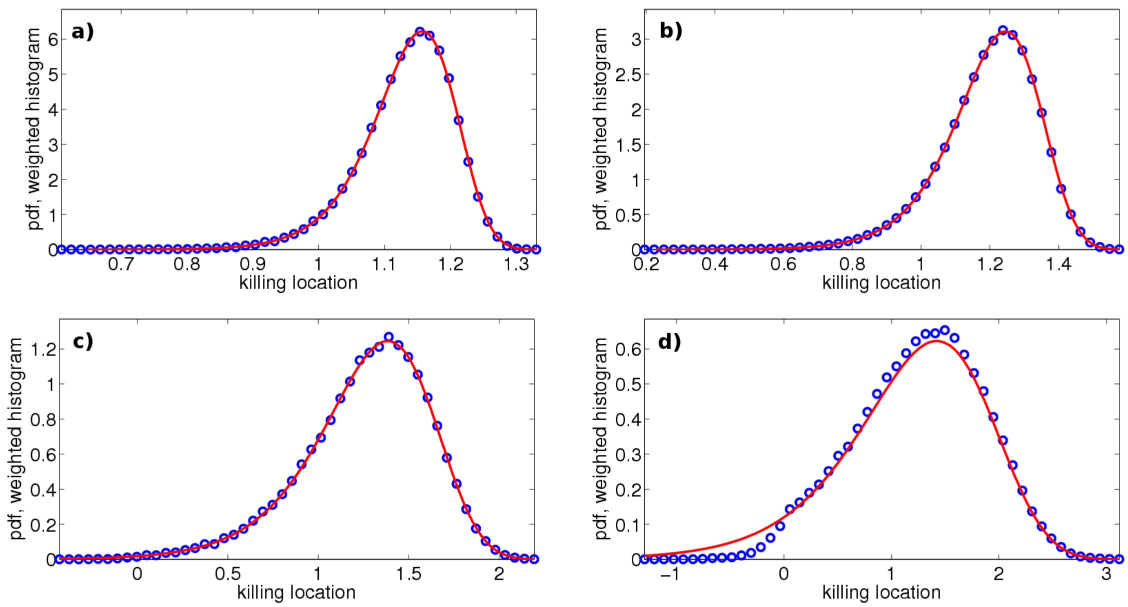

Figure 2: Simulations versus analysis for $\epsilon = .05, .1, .25, .5$, from left to right and top to bottom. We have plotted the analytically-computed pdf from (41– 43) as solid red, and the histogram of the computation is given by blue data points.

saturates quickly (note that the mean changes by a factor of about six over this range, whereas the standard deviation less than doubles). This is somewhat surprising: adding noise to the slow variable does not make the jumping location much more random, whereas it makes the mean of the process change significantly. We discuss this observation further in Section 5 below.

5 Conclusions

We have considered a general killing problem with a small parameter and have showed how to compute the asymptotics for the killing location. This problem arises directly in the study of the dynamics of motor proteins (see Section 1.2.1) and as an approximation for jumps away from a slow manifold in the general context of singularly-perturbed SDE (see Section 1.2.2). In particular, one can now compute asymptotics for motor protein models where the cargo is also subject to thermal fluctuations. As described in Section 1.2.1, the model considered in this paper is the exact model which one would use to describe the motion of one motor on a one-dimensional filament. Interesting problems arise when one considers coupled collections of such motors, see [12, 13]; one could extend the analysis here to cases of that type.

As noted in Section 1.2.2, the current analysis gives a closer approximation for computing “jump locations” in singularly-perturbed SDE asymptotics; previous arguments were only applicable when the slow variable was deterministic (this was done in [7, 12, 11]). Thus the current method, while not the full solution for problems of this type, is an improvement over the current state of the art.

The distribution (20) is known as the Gumbel, Fisher–Tippett, or Extreme Value Distribution [14, 19] in various contexts. It can be obtained as a limit of the minimum order statistic of a

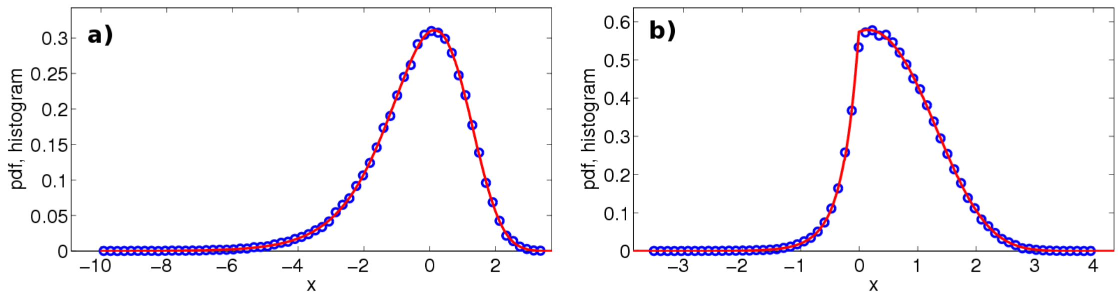

Figure 3: Simulation versus analysis for $\mu = \nu = \rho = \sigma = 1$ and $Z_0 = -10$ or $Z_0 = 0$. Notice that the density is only continuous and not differentiable, when $Z_0 = 0$.

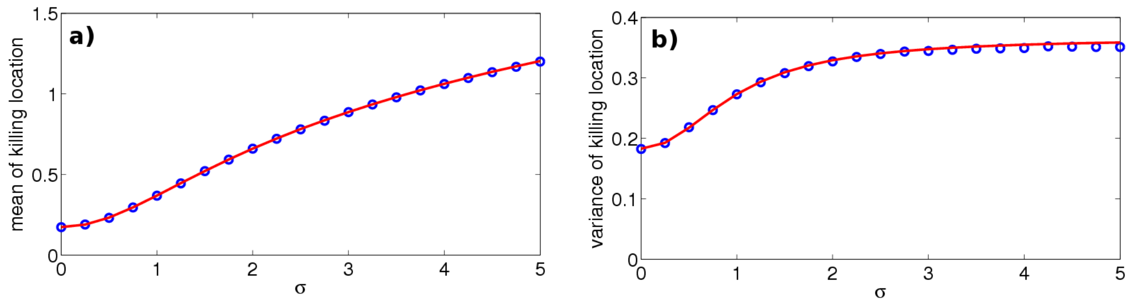

Figure 4: Mean and standard deviation for the killing position in (25, 26). As always, the red curve corresponds to the analytically computed values, and the blue datapoints from direct simulations.

sequence of n i.i.d. random variables. This is not a surprising connection, since it is the c.d.f. for the first time some event occurs, but it is interesting that this law gives the exact limit.

We finish with a comment on a seemingly paradoxical observation made above. As observed in Figure 4, increasing σ increases $\mathbb{E}[X^\epsilon_\zeta]$ without significantly changing the variance of X^ϵ_ζ. At first glance, one might expect that the effect of increasing σ would instead do the opposite, i.e. increase the variance and not change the mean. For example, this would surely be true for the random variable X^ϵ_t for any fixed t if the killing process were turned off. In short, since the average value of X^ϵ_t is independent of σ, we might have expected the location of the jumping-off point to also be independent of σ. As we have seen, however, this is not correct, and it is due to the strong asymmetry in the killing rate. Speaking roughly, for fixed t, $\mathbb{E}[X^\epsilon_t]$ is independent of σ because we are just as likely to get a realization which moves "too slow" as one which moves "too fast" (relative to the mean drift). However, if a realization actually moves much faster than its mean, then it has a possibility of getting further before it survives, since the high killing rate has less time to work. On the other hand, if a realization moves slower than its mean, it spends more time where the killing rate is low, but since the rate is low it is unlikely to jump. Therefore, realizations of the diffusion which move "too fast" have a significantly different effect on the killing location than ones which move "too slow", and this leads to a bias (and increase) in X^ϵ_ζ. Of course, this effect only occurs for a non-constant killing rate and will only become apparent when the killing rate is a rapidly-varying function of space.

6 Acknowledgments

The author is indebted to Richard Sowers, Renming Song, Eric Vanden-Eijnden, and Alex Yong for helpful discussion on these topics.

References

[1] Milton Abramowitz and Irene A. Stegun. *Handbook of mathematical functions with formulas, graphs, and mathematical tables*, volume 55 of *National Bureau of Standards Applied Mathematics Series*. For sale by the Superintendent of Documents, U.S. Government Printing Office, Washington, D.C., 1964.

[2] Bruce Alberts, Alexander Johnson, Julian Lewis, Martin Raff, Keith Roberts, and Peter Walter. *Molecular Biology of the Cell*. Garland Science, 4th edition, 2002.

[3] Andrei N. Borodin and Paavo Salminen. *Handbook of Brownian motion—facts and formulae*. Probability and its Applications. Birkhäuser Verlag, Basel, second edition, 2002.

[4] Anton Bovier, Michael Eckhoff, Véronique Gayrard, and Markus Klein. Metastability in reversible diffusion processes. I. Sharp asymptotics for capacities and exit times. *J. Eur. Math. Soc. (JEMS)*, 6(4):399–424, 2004.

[5] S. C. Chapman, G. Rowlands, and N. W. Watkins. Extremum statistics: a framework for data analysis. *Nonlinear Processes in Geophysics*, 9(5/6):409–418, 2002.

[6] Giovanni Ciccotti, Tony Lelievre, and Eric Vanden-Eijnden. Projection of diffusions on submanifolds: application to mean force computation. *Comm. Pure Appl. Math.*, 61(3):371–408, 2008.

[7] R. E. Lee DeVille, Cyrill B. Muratov, and Eric Vanden-Eijnden. Non-meanfield deterministic limits in chemical reaction kinetics far from equilibrium. *J. Chem. Phys.*, 124(23):Article No. 231102, June 2005.

[8] R. E. Lee DeVille, Cyrill B. Muratov, and Eric Vanden-Eijnden. Two distinct mechanisms of coherence in randomly perturbed dynamical systems. *Phys. Rev. E (3)*, 72(3):031105, 2005.

[9] R. E. Lee DeVille and Eric Vanden-Eijnden. A nontrivial scaling limit for multiscale Markov chains. *J. Stat. Phys.*, 126(1):75–94, 2007.

[10] R. E. Lee DeVille and Eric Vanden-Eijnden. Self-induced stochastic resonance for Brownian ratchets under load. *Commun. Math. Sci.*, 5(2):431–446, 2007.

[11] R. E. Lee DeVille and Eric Vanden-Eijnden. Regular gaits and optimal velocities for motor proteins. *Biophysical J.*, 95(6):2681–2691, September 15 2008.

[12] R. E. Lee DeVille and Eric Vanden-Eijnden. Regularity and synchrony in motor proteins. *Bull. Math. Biol.*, 70(2):484–516, 2008.

[13] Thomas A. J. Duke. Molecular model of muscle contraction. *Proceedings of the National Academy of Sciences of the United States of America*, 96(6):2770–2775, 1999.

[14] Michael Falk, Jürg Hüsler, and Rolf-Dieter Reiss. *Laws of small numbers: extremes and rare events*. Birkhäuser Verlag, Basel, extended edition, 2004.

[15] Michael E. Fisher and Anatoly B. Kolomeisky. The force exerted by a molecular motor. *Proceedings of the National Academy of Sciences*, 96:6597–6601, June 1999.

[16] Michael E. Fisher and Anatoly B. Kolomeisky. Simple mechanochemistry describes the dynamics of kinesin molecules. *Proceedings of the National Academy of Sciences*, 98(14):7748–7753, 2001.

[17] Mark I. Freidlin. On stable oscillations and equilibriums induced by small noise. *J. Statist. Phys.*, 103(1-2):283–300, 2001.

[18] Mark I. Freidlin and Alexander D. Wentzell. *Random perturbations of dynamical systems*. Springer-Verlag, New York, second edition, 1998.

[19] J. B. S. Haldane and S. D. Jayakar. The distribution of extremal and nearly extermal values in samples from a normal distribution. *Biometrika*, 50(1-2):89–94, 1963.

[20] Kiyosi Itô and Henry P. McKean, Jr. *Diffusion processes and their sample paths*. Springer-Verlag, Berlin, 1974. Second printing, corrected, Die Grundlehren der mathematischen Wissenschaften, Band 125.

[21] Ioannis Karatzas and Steven E. Shreve. *Brownian motion and stochastic calculus*, volume 113 of *Graduate Texts in Mathematics*. Springer-Verlag, New York, second edition, 1991.

[22] James P. Keener. *Principles of applied mathematics*. Perseus Books, Advanced Book Program, Cambridge, MA, revised edition, 2000. Transformation and approximation.

[23] Anatoly B. Kolomeisky and Michael E. Fisher. A simple kinetic model describes the processivity of myosin-V. *Biophysical Journal*, 84:1642–1650, 2003.

[24] B. J. Matkowsky and Z. Schuss. The exit problem for randomly perturbed dynamical systems. *SIAM J. Appl. Math.*, 33(2):365–382, 1977.

[25] Cyrill B. Muratov, Eric Vanden-Eijnden, and Weinan E. Self-induced stochastic resonance in excitable systems. *Phys. D*, 210(3-4):227–240, 2005.

[26] Bernt Øksendal. *Stochastic differential equations*. Universitext. Springer-Verlag, Berlin, sixth edition, 2003. An introduction with applications.

[27] Robert E. O'Malley, Jr. *Singular perturbation methods for ordinary differential equations*, volume 89 of *Applied Mathematical Sciences*. Springer-Verlag, New York, 1991.

[28] R. B. Paris and D. Kaminski. *Asymptotics and Mellin-Barnes integrals*, volume 85 of *Encyclopedia of Mathematics and its Applications*. Cambridge University Press, Cambridge, 2001.

[29] Donald R. Smith. *Singular-perturbation theory*. Cambridge University Press, Cambridge, 1985. An introduction with applications.

[30] Ronald D. Vale and Ronald A. Milligan. The way things move: Looking under the hood of molecular motor proteins. *Science*, 288:88–95, 2000.

[31] Ferdinand Verhulst. *Methods and applications of singular perturbations*, volume 50 of *Texts in Applied Mathematics*. Springer, New York, 2005. Boundary layers and multiple timescale dynamics.

A Exact Computation of Moments

We will follow the standard approach for the Fisher-Tippett distribution, which is slightly modified for this case (see e.g. [5]). We start with the cumulants:

$$c_k := \int_{-\infty}^{\infty} x^k A \exp\left(Bx - \frac{A}{B}e^{Bx}\right)\, dx.$$

We make the change of variables

$$y = Ae^{Bx}/B, \quad dy = By\,dx,$$

so

$$c_k = \int_0^\infty (\log By/A)^k \frac{e^{-y}}{B^k}\,dy.$$

Recall that

$$\Gamma^{(n)}(1) = \int_0^\infty e^{-t}(\log t)^n\,dt,$$

and this gives

$$c_k = B^{-k}\sum_{j=0}^{k}\left(\begin{array}{c}k\\j\end{array}\right)(\log B/A)^{k-j}\Gamma^{(j)}(1).$$

Finally, to obtain the kth moment, we write

$$m_k = \sum_{l=0}^{k}\left(\begin{array}{c}k\\l\end{array}\right)(-m_1)^{k-l}c_l, \quad m_1 = c_1.$$

B Solution to (36) using Bessel functions

We want to solve

$$\frac{1}{2}f'' + f' + Ae^{Bx}f = 0. \tag{36}$$

Writing

$$f(x) = e^{-x}y(\alpha e^{\beta x}) \tag{44}$$

gives

$$\alpha^2\beta^2 e^{(2\beta-1)x}y''(\alpha e^{\beta x}) + \alpha\beta^2 e^{(\beta-1)x}y'(\alpha e^{\beta x}) + (2Ae^{(B-1)x} - e^{-x})y(\alpha e^{\beta x}) = 0.$$

Writing $\xi = \alpha e^{\beta x}$ and multiplying through by e^x/β^2 gives

$$\xi^2 y''(\xi) + \xi y'(\xi) + \left(\frac{2A}{\beta^2}e^{Bx} - \frac{1}{\beta^2}\right)y(\xi).$$

Choosing $\alpha = \sqrt{2A/B^2}$ and $\beta = B/2$ gives

$$\xi^2 y''(\xi) + \xi y'(\xi) + (\xi^2 - 4/B^2)y(\xi) = 0,$$

whose solution is the Bessel function

$$y(\xi) = J(2/B, \xi),$$

and from (44),

$$f(x) = e^{-x}J\left(2/B, \sqrt{8AB^{-2}e^{Bx}}\right).$$